DESIGN AND TESTS OF AN HELICOPTER ROTOR BLADE WITH EVOLUTIVE PROFILE

J.J. Thibert
Office National d'Etudes et de Recherches Aérospatiales (ONERA)
92320 Châtillon (France)
and J.M. Pouradier
Société Nationale Industrielle Aérospatiale (SNIAS)
Division Hélicoptères, 13722 Marignane (France)

Abstract

In 1974, ONERA and AEROSPATIALE undertook jointly a research program to improve helicopter rotor aerodynamics and particularly to design optimized blades for future machines. This paper is a synthesis of the results obtained during the design process of a blade with evolutive profile.

In the first part, the design methodology of a new family of airfoils sections covering a range of thickness to chord ratios from 6 to 13 per cent is presented and the performance of these airfoils deduced from tests in the S3 Modane wind tunnel are compared with those of other known airfoils.

In the second part the results obtained on model rotors and in flight on a SA365 "Dauphin" helicopter will be presented and analyzed. The use of the OA family gives an improvement of the rotor performances in hover and avandcing flight and a reduction of the pitch control loads. The flight envelope has also been increased with these new airfoils. All these results will help us to set up the specifications of the future airfoil generation.

List of symbols

b : number of blades
c : chord (m)
C_D : airfoil drag coefficient
C_L : airfoil lift coefficient
C_m : airfoil pitching moment coefficient
C_T : rotor lift coefficient $C_T = \dfrac{F_z}{\rho S U^2}$
$\bar{C}$: rotor reduced power $\bar{C} = \dfrac{100\,W}{\frac{1}{2}\rho S \sigma U^3}$
t/C : airfoil thickness to chord ratio
FM : rotor figure of merit $FM = \dfrac{F_z^{3/2}}{\sqrt{2\rho S}} \dfrac{1}{W}$
F_x : rotor propulsive force (N)
F_z : rotor lift (N)
L/D : lift to drag ratio
M_{dd} : airfoil drag divergence Mach number
M_T : Mach tuck
R : rotor radius (m)
S : rotor disc area $S = \pi R^2$ (m^2)
U : circumferential speed (m/sec)
V : flight speed (m/sec)
W : rotor power (W)
$\bar{X}$: rotor drag coefficient $\bar{X} = \dfrac{-100\,F_x}{\frac{1}{2}\rho S \sigma U^2}$
α : airfoil incidence
α_q : rotor shaft angle (degrees)
Λ : rotor advance ratio $\Lambda = V/U$
η : rotor lift to drag ratio $\eta = \dfrac{F_z V}{W - F_x V}$
ρ : air density (kg/m^3)
σ : rotor solidity $\sigma = \dfrac{bC}{\pi R}$

I. Introduction

Most of the airfoils used on the blades of to days' operating helicopters were designed in the 30's. This is due to the fact that if aerodynamics have always been considered of the first importance for fixed wing aircraft designs, it was not true for helicopters. In fact, since the end of the second world war, which was the beginning of this new industry, until the end of the 60's, the improvement of helicopters performances was due to mechanical progresses and mainly to the utilization of turbines. For ten years however, manufacturers have made big efforts to improve the aerodynamics of their machines in order to increase cruise speeds and payloads and to decrease the fuel consumption. For the main rotor the use of composite materials allows the design of blades with a spanwise evolution of the airfoil's sections and the progress made over the last few years for wings can be applied to these new blades.

It is in this framework that ONERA undertook in 1974 the design of new airfoils for helicopter blades. Design objectives for these airfoils have been set up by AEROSPATIALE in order to improve the rotor performances of its new machines.

II. Historical background

The examination of the airfoils used on the blades (Fig. 1) shows the same evolution (with some delay) than for the wings. On the very first machines designed between

Work performed with the financial support of DRET and STPA.

1900 and 1930 thin airfoils were used while between 1930 and 1945 airfoils were chosen in the famous Göttingen or NACA series. During the 50's the vogue of laminar flow airfoil sections reaches helicopter and the NACA 6 serie and the NACA H serie with reflex camber were used. However laminar flow airfoil sections were unsuccessful, due to the presence of cross flow on the blade which destabilize the laminar boundary layer and also due to the very poor stall characteristics of these airfoils. So in the 60's classical NACA or modified NACA sections were again chosen. It can be outlined that during all this period metallic blades had the same airfoil section all over the span.

However since the begining of the 70's, researches have been made by most of the manufacturers to design new airfoils adapted for helicopters. These new airfoils have better performances than the old ones but are not yet widely used on the helicopters operating to days.

Figure 2 shows that on the french helicopters the NACA 0012 has been widely used. Only the recent machines like the SA 330 J version of the PUMA, the twin engines SA 365 N and SA 366 G from the DAUPHIN serie have tapered blades with airfoils which are not NACA or modified NACA sections. For the twin engines AS 355 the blade is untapered but uses also a new airfoil.

III. Design objectives for helicopter rotor airfoils

The recent evolution towards tapered blades can be easily explained when we see the iso-Mach and the iso-angle of attack lines through the rotor disc drawn on Fig. 3 for a typical forward flight case. The combination of rotating and advancing speeds leads on the advancing side of the disc (azimuth angle varying between 0 and 180°) to a spanwise evolution of the relative Mach number between 0.2 near the hub up to 0.85 at the tip. On the retreating side (azimuth angle varying between 180 and 360°) the Mach numbers are lower and vary between 0.4 at the tip and 0., and sometimes negative values in the reverse flow region, near the hub. So to maintain the roll balance of the rotor, angles of attack and C_L are small on the advancing side and high on the retreating side of the rotor disc. Airfoils during a cylce are alternatively submitted to low angles of attack with high Mach numbers and high angles of attack with low Mach numbers. Mach numbers and angles of attack levels vary with the spanwise position of the airfoil section, so the optimization of the rotor leads to the design of blades with a spanwise thickness evolution. An another flow regime for the blade is encountered in hover flight for which there is no Mach number variation with azimuth angle and consequently the level of C_L is constant ($M_o \sim 0.6$, $C_L \sim 0.6$, at the tip).

With this analysis of the different flow regimes, it is possible to quantify the two dimensional airfoil characteristics which have the greatest impact on rotor performances and loads for the three main flight areas :

- advancing flight
- hover
- maneuver.

Fig. 4 shows the design objectives for the airfoils sections along the blade settled by AEROSPATIALE. The blade has been divided in three parts :

- inboard sections $r/R < 0.8$
- intermediate sections $0.8 < r/R < 0.9$
- tip sections $r/R > 0.9$.

Two sets of specifications have been set up for the inboard and the tip sections. One is oriented toward the research of high lift capability while the other is oriented to the research of high performances at high speed. The figures in Fig. 4 show that the objectives are much more higher than the performances of the NACA 0012 since the C_L Max of this airfoil at $M_o = 0.4$ is 1. and its Mach drag divergence at zero lift is 0.79 (values deduced from tests in the S3 Modane wind tunnel with free transition and a Reynolds number of $7 \times M_o \times 10^6$). It can be outlined that the C_{mo} requirement of AEROSPATIALE is extremely severe even for the inboard sections in order to avoid the torsion effects on the blade and to minimize the efforts on the control rods.

IV. Design methodology of the OA airfoil family

On the basis of these requirements ONERA designed 5 airfoils. Their thickness to chord ratios vary from 6 to 13 percent. The first airfoil designed was for the section 2 of the blade.

4.1. Airfoil for the 85 per cent spanwise section of the blade

The section 2 of the blade is located at about 85% of the span and the thickness required is approximately 9%. The airfoil for this section has been called OA 209 and it has already been presented in details [1]. It was designed with an inverse method [2]. The prescribed pressure distribution around the airfoil was chosen for $C_L \sim 0$ to insure a low drag level at high speed and a small pitching moment coefficient. The main performances of the OA 209 airfoil deduced from wind tunnel tests made in the S3 Modane wind tunnel on a 210 mm chord model are shown Fig. 5. These performances are the C_L max for Mach numbers lower than 0.5, the Mach drag divergence for constant levels of C_L for Mach numbers greater than 0.5 and the zero lift pitching moment coefficient evolution with Mach number. The objectives of Fig. 4 have been met for the M_{dd} at $C_L \sim 0$ which is 0.85 and for the C_{mo} which is extremely low even at high Mach numbers. The L/D at $M_o = 0.6$, $C_L = 0.6$ is 75 and the C_L max is 1.27 for $M_o = 0.3$ and 1.21 for $M_o = 0.4$, values a little lower than the specifications but high for a 9 per cent

thick airfoil. Compared to the NACA 0012 the gains are important :

ΔC_L max = + 11% at $M_o = 0.3$; + 21% at $M_o = 0.5$
ΔM_{dd} = + 0.06 at $C_L = 0$
$\Delta L/D$ = + 25% for $M_o = 0.6$; $C_L = 0.6$.

These overall good performances lead us to take this airfoil as the basic airfoil for the new family.

4.2. Airfoils for the blade tip sections

Two sets of specifications have been set up for the tip of the blade. In the first one emphasis has been made on the high lift capability in order to delay the stall on the retreating blade. So to keep the good performances of the OA 209 at high angles of attack which are due to its leading edge contour, the forepart of this airfoil has been kept while an affinity on the abscissa has been made on the rear part in order to get a 7% thick airfoil to increase performances at high Mach number (Fig. 6).

This technique moves the maximum thickness forward which has a benefit effect for high lift capabilities and counterbalances the negative effect of the decrease in thickness. This design method reduces the amount of camber, unloads the rear part of the airfoil and so gives more nose up pitching moment coefficient. The airfoil obtained by this way has been called OA 207.

In the second set of specifications the high Mach numbers performances have been outlined which led us to choose a 6% thick airfoil called OA 206. For this airfoil the method used by the NACA to generate airfoils sections has been selected. The thickness distribution of the basic airfoils OA 209 has been kept with an affinity to get a maximum thickness of 6% (Fig. 6). Compared to the OA 207, the OA 206 has a lower thickness and its maximum thickness is located backward and so should exhibit higher Mach drag divergence and a lower drag level. To meet the C_L max requirement at $M_o = 0.4$ some amount of camber is necessary and the mean line of the OA 206 has been derived from the NACA 131 serie.

The OA 207 and OA 206 theoretical performances have been calculated with a transonic viscous code [3]. This code has been calibrated with the tests results of various airfoils made in the S3MA wind tunnel. These comparisons show that the M_{dd}, the drag level and the C_{mo} can be estimated with confidence. The C_L max however cannot be computed and it has been evaluated on the basis of the estimation of the K_p mini on the upper surface at the stall deduced from the wind tunnel tests [4].

The performances of these airfoils are compared Fig. 8 at those of some other known thin airfoils. These airfoils are the symmetrical NACA 0006, the Boeing-Vertol VR 3006–0.7 and VR8 which are derived from NACA series like the AEROSPATIALE SA 13106–0.7. The contours of these airfoils are drawn Fig. 7 while the performances found in [5] and [6] are presented Fig. 8 in term of C_L max at $M_o = 0.4$, M_{dd} for $C_L \sim 0$, C_{mo} at $M_o = 0.4$ and drag level at $M_o = 0.6$, $C_L = 0.6$.

As it was expected the OA 207 has a better C_L max at $M_o = 0.4$ (1.1) than the OA 206 (0.97) and its M_{dd} is lower (0.895 versus 0.91). The two airfoils have also a very low and positive C_{mo}. Compared to the other sections, these airfoils have a better M_{dd} and the OA 207 has the highest C_L max while for the OA 206 the value is about the same than for the other 6% thick airfoils. Their C_{mo} are also better than those of the other cambered sections. These two thin airfoils have overall good performances and give substantial gains for high Mach number compared to the OA 209.

4.3. Airfoils for the blade inboard sections

The main requirement for the inboard part of the blade is high lift capability at low Mach numbers to avoid stall on the retreating side of the rotor disc. However the value of the C_L max required varies with the helicopter class and its mission. So two sets of specifications have been set up by AEROSPATIALE in order to get a wider choice of airfoils for its new blades. One of this set requires an airfoil with overall good performances in all the flight areas while for the second one the airfoil has to have a very high maximum lift at $M_o = 0.4$. The airfoils designed to meet these objectives have been called respectively OA 212 and OA 213. For the OA 212 the design method of the OA 206 has been utilized. This airfoil has the same thickness distribution than the OA 209 with an affinity of 4/3 to get a 12% thick airfoil (Fig. 9) ; so the good performances of the OA 209 for low C_L and high Mach numbers can be preserved. Different mean lines have been tested in order to achieve a theoretical evolution of the maximum leading edge expansion with lift coefficient giving for the level of C_L required a K_p mini lower than the stall value deduced from an experimented correlation [4]. The mean line selected is derived from those of the NACA 6 serie with some amount of reflex on the rear part to reduce the C_{mo}. To achieve higher lift coefficient at $M_o = 0.4$ with low C_{mo}, computations show that it was necessary to modify the thickness distribution ; so the OA 213 airfoil has been designed with an inverse method [2]. The design pressure distribution was choosen for $M_o = 0.5$ and $C_L = 1$ and has been derived from those of the OA 212 for the same condition with a reduction of the leading edge expansion. Some modifications near the trailing edge of the airfoil computed by the inverse method have been made to include a trailing edge tab and so to get the final OA 213. The OA 212 and OA 213 airfoils have been tested in the same conditions than the other airfoils in the S3 Modane wind tunnel. If there is only a few publications concerning thin airfoils there is a lot for 12% thick airfoils. Some have been selected for comparisons. Their contours are drawn

Fig. 10. Their performances are compared with those of the OA 212 and OA 213 on Fig. 11. The NACA 0012, "NACA cambré" and SA 13112 airfoils have also been tested in the S3MA wind tunnel while the performances of the other have been found in [5] and [6]. The symmetrical NACA airfoils have poor maximum lift capabilities while the V 43012–1.58 has a very high C_L max at $M_o = 0.3$ but its M_{dd} is only 0.65. The other airfoils have high M_{dd} but relatively low C_L max (NPL 9615, NPL 9660, NACA cambré, SA 13112), or high C_L max but moderate M_{dd} (VR7). The OA 212 shows a good compromise for all the flight areas and as it was expected the OA 213 has a better C_L max at $M_o = 0.3$ but a lower M_{dd}. It can be outlined that these two airfoils have a very low C_{mo} without special tab deflection. For Mach numbers 0.3 and 0.5 the OA213 airfoil has not much more maximum lift than the OA 212 but for $M_o = 0.4$ the curves of Fig. 12 show that the difference is important. The C_L max is 1.37 for the OA 212 and 1.55 for the OA 213.

V. Review of the performances of the OA family

The five airfoils which constitute the OA family are drawn Fig. 13 and their C_L max at $M_o = 0.3$ and 0.5 and their M_{dd} are plotted Fig. 14 versus the thickness to chord ratio. This family covers a wide range of M_{dd} from 0.75 up to 0.91 and also of C_L max from 0.97 to 1.46 at $M_o = 0.3$. So these airfoils allow the definition of blades with potential performances much more better than the classical ones equipped with the NACA 0012, the performances of which are also plotted Fig. 14.

On Fig. 15 and 16 the OA family is compared at two other airfoil families, one designed by AEROSPATIALE some years ago and used on the SA 330 Puma [7] and the other designed by Boeing-Vertol. The comparison is made Fig. 15 in term of C_L max for Mach numbers 0.3, 0.4 and 0.5. The OA family is better than the SA family for all the ranges of thicknesses and Mach numbers and also better than the VR family for the small thicknesses but as it has been already pointed out the VR family has very good C_L max for $t/c = 0.12$ especially at $M_o = 0.5$ while at $M_o = 0.4$ the OA 213 has a C_L max much more higher than the others. For the M_{dd} at $C_L = 0$ and the Mach tuck (defined as the Mach number for which $dC_{mo}/dM_o = -0.25$) Fig. 16 the OA has also better performances. It is difficult to compare the L/D of the VR family with the others because the tests have not been made at the same Reynolds number but nevertheless the VR8 has a very low drag level for $M_o = 0.6$ $C_L = 0.6$. As a conclusion this new family has reached most of the AEROSPATIALE specifications and covers a wide range of performances. These five airfoils allow the design of blade for helicopters of different classes and missions.

VI. Rotor tests with the OA 209 airfoil

In view of the satisfactory results obtained in two-dimensional flow on the OA 209 airfoil, the improvement of rotor performances anticipated with the use of this airfoil have been estimated using a simplified performance calculation method [8].

The aircraft studied was the SA 360 "Dauphin" which has a maximum weight of 3000 kg and can carry 9 passengers plus the pilot at a maximum speed up to 310 km/hr. The 11.50 m diameter rotor on the production version aircraft is equipped with a NACA 0012 airfoil with a 0.350 m chord and the theoretical aerodynamic twist is –8°.

Computations showed that the following gains could be achieved by replacing the NACA 0012 airfoil by the OA 209 :

– in hover flight : at constant rotor power, a 2 to 5% increase of rotor lift, according to the rotor load level ;

– in forward flight : a 7% power saving at sea level and 12% at 2000 m.

These gains are due to the following reasons :

Flight conf. / Airfoil data	Hover flight	Forward flight
C_L/C_D at $M_o = 0.6$ and $C_L = 0.6$	– improved blade tip L/D → + 2 to 5% on F_Z at iso W	
C_L max at $M_o = 0.4$ and C_L/C_D at $M_o \leq 0.4$ and $C_L \sim C_L$ Max		– delayed retreating blade stall → +5% on rotor lift at stall limit and improved vibratory level under heavy loads – improved forward and rearward blade L/D under heavy loads → –5% on W in altitude
M_{dd} at $C_L = 0$		– decreased drag on advancing blade → – 7% on W at high speed
C_m		→ decreased dynamic loads on blades and control linkages ; reduced control operating loads

These predicted benefits were confirmed in 1977 by flight tests on a SA 360 "Dauphin" equipped with the OA 209 airfoil. The full tests results have already been presented [1].

In hover flight, the iso-power lifted weight was increased by about 2%. The forward flight envelope was appreciably extended ; the rotor lift was increased by about 10%, whatever the airspeed, at maximum engine power (Fig. 17). Fig. 18 shows typical constant power airspeed gains, ranging from 5 km/hour at sea level up to 50 km/hour at 4000 m in standard atmosphere. These better performances are due to the rotor L/D improvement.

A static load analysis of the control linkage showed an appreciable reduction in lateral stick loads, allowing the flight envelope to be enlarged for a light weight aircraft in the event of a hydraulic control system failure (Fig. 19).

The forward flight vibration level versus altitude or load factor was significantly reduced with the OA 209 airfoil (Fig. 20). This is a logical result since the vibration level is related to the drop in the rotor L/D under heavy load or for high advance ratios. On the basis of these satisfactory results, the OA 209 airfoil was adopted for the production use on the twin-engine SA 355 helicopter.

VII. Tests on rotors with thickness tapered blades

Various studies have shown that tapering the rotor improves high speed and moderate loads performances, but often with penalty in stall limit due to the low C_L max of thin airfoils[9]. To overcome this drawback, the OA 207 airfoil was designed to have both a high M_{dd} and about the same C_L max at $M_o = 0.4$ than the NACA 0012. In order to confirm that this objective was met two rotors were tested in the large ONERA S1MA wind tunnel. These rotors differed only in the airfoil spanwise distribution : one had a constant OA 209 profile while the second had the OA 209 profile refined into the OA 207 profile at the tip [4]. The wind tunnel test section is 8 m in diameter, allowing tests of rotors up to 4 m in diameter. For the test runs, the maximum wind speed in the test section is 132 m/sec, well above the airspeed range of existing helicopters. The rotor shaft may be tilted from +25° to −95° from vertical position, thus covering power-on and power-off forward flight and quasi-hovering flight (rotor shaft in axial position). The circumferential speed of 210 m/sec (i.e. of the same order of magnitude as that encountered on helicopters) allows compressibility phenomena to be correctly represented.

Tests were conducted on two four bladed rotors having a diameter of 4 m, a blade chord of 0.140 m and a theoretical aerodynamic twist of −8.3°. The blades definitions are summarized in the following table.

Rotor 6A	OA 209 profile : constant from 0.2 R to R
Rotor 6B	OA 209 profile : constant from 0.2 R to 0.8R then linearly refined from 0.8 R (OA 209) to R (OA 207)

Tests results showed that the objectives were achieved. No detrimental effects were observed in hover flight, even for high rotor loads, for rotor tip Mach number up to 0.64 (as it is the case for the Aerospatiale main rotors). Above this value, for high rotor loads ($C_T/\sigma > 0.1$) the OA 207 drag increases and a slight performance drop is observed with the tapered blades (Fig. 21). In forward flight, thickness taper did not shows appreciable improvement until the advancing blade tip velocity exceeds Mach 0.86. Above this value, for moderate rotor loads, the high M_{dd} of the OA 207 airfoil delays drag divergence and the performance gains rapidly increase (Fig. 22). For high rotor loads, the tips for the forward and rearward blade on the tapered rotor reach the drag divergence value and the performance gains decrease. Under no circumstances, however, the performances of the tapered rotor are lower than those of rotor 6A. No dynamic problems were encountered with these rotors.

VIII. Design and flight tests of a rotor blade with an evolutive profile

Based on the satisfactory tests results obtained in wind tunnel and in flight with the OA airfoils, the decision was made to equip the new "Dauphin" version (SA 365 N) with a blade having a spanwise evolution of the airfoil's sections, sections taken in the OA family. The OA 212 airfoil was available at this time, and it was decided to use it in the blade design to improve rotor performance under heavy loads. For the same reason, the blade twist was slightly increased (−8° to −10°) as was the chord dimension (365 mm to 385 mm) over the initial production blade values. Fig. 23 shows the main characteristics of this new "third generation" blade. The OA 212 profile runs from the blade shank to 0.75 R station, after which it is gradually tapered to the OA 207 at the blade tip (evoluing through the OA 209 at 0.9 R).

The performances of the third generation blades were compared with those of the NACA 0012 airfoil blades during flight tests conducted in 1978 on a SA 365 C [4] [10].

The comparison of the hover mode lift efficiency versus rotor load (see curves plotted Fig. 24) shows that the lift efficiency of the OA rotor is about 5% higher than for the NACA 0012 rotor. This gain represents an increase of about 100 kg in the iso-power maximum weight capability.

The two types of blades were not fully compared on the same aircraft in forward flight, since the new blades had not yet been completely fatigue-substantiated at the test date. However the improvements noted at airspeeds up to 120 knots (Fig. 25) seem to confirm the expected 3% drop in specific fuel consumption at best-range cruising speed.

In the absence of flight comparisons, Fig. 26 shows a calculated evaluation of the anticipated forward flight performance gains obtained with the OA airfoil family. The figure compares the L/D ratios of an OA rotor and an another one having the same geometry but a constant spanwise NACA 0012 section. The OA rotor gives an appreciable improvement in efficiency compared to the NACA 0012 one over much of the flight envelope. The differences between the two rotors are

References

(1) J.J. Thibert and J. Gallot — A new family for rotor blades, Paper presented at 3th European Rotorcraft and Powered lift Aircraft Forum, 1977. TP ONERA 1977-131.

(2) Y. Morchoisne — Méthode de calcul inverse en écoulement compressible, AAAF, 12e Colloque d'Aérodynamique Appliquée (1975).

(3) J. Bousquet — Calculs bidimensionnels transsoniques avec couche limite, AAAF, 11e Colloque d'Aérodynamique Appliquée (1974).

(4) J.J. Thibert and J. Gallot — Advanced Research on Helicopter blade airfoils, Paper presented at 6th European Rotorcraft and Powered Lift Aircraft Forum, Sept. 1980.

(5) L.U.Dadone — Rotor airfoil optimization : an understanding of the physical limits, Paper presented at 3th Annual AHS Forum, May 1978.

(6) U.S. Army helicopter design datcom, Volume I, airfoils. Boeing Doc No 0210-1197-1, May 1976.

(7) J. Renaud and F. Nibelle — Effects of the airfoil choice on rotor aerodynamic behaviour in forward flight. Paper presented at the 2nd European Rotorcraft and Powered Lift Aircraft Forum, 1976.

(8) J. Gallot — Helicopter Rotor Loads Prediction Methods. AGARD CP No 122, 1973.

(9) R.G. Benson, L.U. Dadone, R.E. Gormont and G.R. Kohler — Influence of airfoils on stall flutter boundaries of articulated helicopter rotors. 28th annual Forum of the American Helicopter Society, May 1972.

(10) P. Roesch — Aerodynamic design of the Aerospatiale AS 365 N - Dauphin 2 helicopter. Sixth European Rotorcraft and Powered Lift Aircraft Forum, Sept. 1980.

(11) L.U. Dadone — Design and analytical study of a rotor airfoil. NASA CR 2988, 1978.

(12) R.E. Gormont — A mathematical model of unsteady aerodynamics and radial flow for application to helicopter rotors. USAAMRDL TR 72-67, May 1973.

(13) R.G. Carlson, R.H. Blackwell, G.L. Commerford and P.H. Mirick — Dynamic stall Modeling and Correlation with Experimental Data on Airfoils and Rotors. AHS/ NASA Ames Specialists' Meeting on Rotorcraft Dynamics, Feb. 1974.

(14) T.S. Beddoes — A synthesis of unsteady aerodynamic effects including stall hysteresis. 1st European Rotorcraft and Powered Lift Aircraft Forum, Southampton (England), September 1975.

(15) L.E. Ericsson and J.P. Reding — Dynamic stall analysis in Light of Recent Numerical and Experimental Results. AIAA Paper 75-26 January 1975.

(16) W.J. McCroskey — Prediction of unsteady separated flows on oscillating airfoils. AGARD Lecture Series No 94 Three Dimensional and Unsteady Separation at High Reynolds Numbers.

(17) J. Renaud and J. Coulomb — 2D simulation of unsteady phenomena on a rotor. Fourth European Rotorcraft and Powered Lift Aircraft Forum, Stresa (Italy),Sept. 1978.

(18) L.U. Dadone — Observation on the dynamic stall characteristics of advanced helicopter rotor airfoils. NASA conference publication 2045 Vol. I, Part 2.

(19) E. Szechenyi — An experimental study of the dynamic forces acting on fixed and vibrating two-dimensional aerofoils. Third European Rotorcraft and Powered Lift Aircraft Forum, Aix-en-Provence (France), Sept. 1977.

1907-1930	THIN AIRFOILS	
1930-1945	GOETTINGEN OR NACA SECTIONS	
	KELLETT KD1 (1935)	GOETTINGEN 770
	SIKORSKY YR4 (1943)	NACA 0012
		NACA 23015
	PIASECKI PV2 (1945)	NACA 0012.6
		NACA 23012.6
		NACA 23015
1950-1960	LAMINAR AIRFOILS	
	SERIE 6 (65-412 - 63A012 - 63A015)	
	SERIE H	(9 H 12)
1960-1970	NACA OR MODIFIED NACA SECTIONS	
1970	DESIGN OF NIEW SECTIONS FOR ROTOR BLADES	

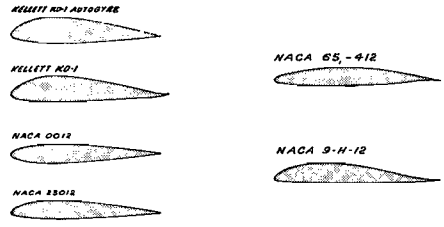

Fig. 1 — Helicopter airfoils sections history.

especially important at high advance ratios and at high rotor loads : this is in agreement with the higher capabilities in C_L max and L/D for high C_L of the OA airfoils.

IX. Rotor tests with the OA 213 and OA 206 airfoils

In an attempt to further improve rotor performances, the OA airfoil family has been completed with a new tip section (OA 206) and by a new main section (OA 213). Two rotors are scheduled to be tested in the ONERA S1 Modane wind tunnel to assess the interest of these two airfoils. In order to evaluate separately the influence of each airfoil on rotor performance, they were consecutively included in the rotor design. The reference for comparison is the rotor 6A, described before. Rotor 7A is defined using airfoils OA 213 and OA 209, while rotor 7B is obtained by tapering rotor 7A and so using airfoils OA 213, OA 209 and OA 206. The profile distribution on rotor 7A was defined to achieve the highest possible stall limit at moderate airspeeds ($V \simeq 150$ km/hour, i.e. $\Lambda \simeq 0.2$ for $U = 210$ m/s) without reaching divergence before 340 km/hour (i.e. $\Lambda \simeq 0.45$ for $U = 210$ m/s) at $C_D/\sigma = 0.07$. The airspeed value of 340 km/hour was selected as being attainable by fast helicopters during the next decade. On the basis of these requirements, the rotor 7A was designed as follow :

- OA 213 section from 0.2 R to 0.75 R
- linear tapering from 0.75 R (OA 213) to 0.9 R (OA 209)
- constant OA 209 section from 0.9 R to R

Rotor 7B was derived from rotor 7A as follow :

- OA 213 section from 0.2 R to 0.75 R
- linear tapering from 0.75 R (OA 213) to 0.9 R (OA 209)
- linear tapering from 0.9 R (OA 209) to R (OA 206).

Performances calculations for these two rotors show that the following improvements can be expected :

- Rotor 7A : a 10% increase of the rotor stall limit at $\Lambda = 0.2$ compared with rotor 6A (Fig. 27) without affecting the power under moderate loads at advance ratios up to 0.45.

- Rotor 7B : improved rotor performance and reduced stressing of the blades and control linkage at high speeds by comparison with rotor 7A, while maintaining appreciably higher performances than rotor 6A under heavy loading and at moderate speeds.

X. The next generation of airfoils

A review of past trends in airfoil design is helpful in attempting to predict future developments. Up to the 1960's, helicopter rotors were almost exclusively equipped with symmetrical airfoils, primarily the NACA 0012. The low C_L max of these airfoils resulted in a relatively low rotor stall limit. The first significant event was therefore the introduction of cambered sections having high C_L max values. These airfoils improved rotor performance, but also resulted in higher stresses in the blades and in the control linkage. The next significant event was the appearance of transonic airfoils, which present much improved maximum lift and drag divergence values while maintaining moderate moment coefficients. These airfoils significantly increased rotor performance.

However, it seems that it is physically no longer possible to obtain substantial improvements for the lift and drag divergence values of these airfoils without sacrificing the low C_m requirements [5]. This would result in heavy stress penalties in the blades and the control linkage. It will therefore be necessary to design a new type of airfoils. One possible choice is the "unsteady" airfoil. In forward flight, the azimuthal variations of relative speed, sweep angle and angle of attack give rise to unsteady phenomena. Three unsteady effects illustrated Fig. 27 are of considerable importance for rotor behaviour :

- the stall delay for C_m and C_L (dynamic stall occurs at higher angle of attack than static stall),
- the possibility to obtain C_L values in unsteady flow higher than the static C_L max,
- aerodynamic damping on the pitch axis.

Of these three effects, only the sign of the pitch axis aerodynamic damping has been related to a steady airfoil characteristic : the type of static stall [11].

Airfoils designed on the basis of unsteady criteria should thus permit significant rotor performance improvements. Unfortunately, in spite of a large number of studies (e.g. [12] to [19]) unsteady phenomena are still too poorly understood to be used for the design of airfoils. Further researches will be required in this area.

XI. Concluding remarks

New airfoils have been designed with better C_L max and M_{dd} values than the conventional airfoils. Most of the two-dimensional characteristics of these airfoils can be estimated using viscous transonic computer codes. However, the maximum lift coefficient can only be computed by separated flow analysis.

The use of these airfoils has resulted in improved rotor performances : increased hover lift efficiency, better L/D ratios at high speeds and heavy loads. For helicopter applications, several options are thus made feasible :

- increased maximum gross weight
- increased take off weight
- increased maximum speed
- increased maneuverability.

Further improvements in helicopter rotor performance will require the development of airfoils based on unsteady criteria.

 Alouette 2	SA 318	1955	NACA 0012
 Alouette 3	SA 316	1959	NACA 63A011.5
 Lama	SA315	1969	NACA 63A011.5
 Super Frelon	SA321	1962	NACA 0012
 Puma	SA330G	1965	NACA 0012
	SA330J	1975	Famille SA 131
 Gazelle	SA 341	1967	NACA 0012
 Dauphin 2	SA 360	1972	NACA 0012
	SA365C	1975	NACA 0012
	SA365N	1979	Famille OA
 Ecureuil	AS350	1974	NACA 0012
	AS355	Fin 1979	OA 209

Fig. 2 – Airfoil sections used on french helicopters.

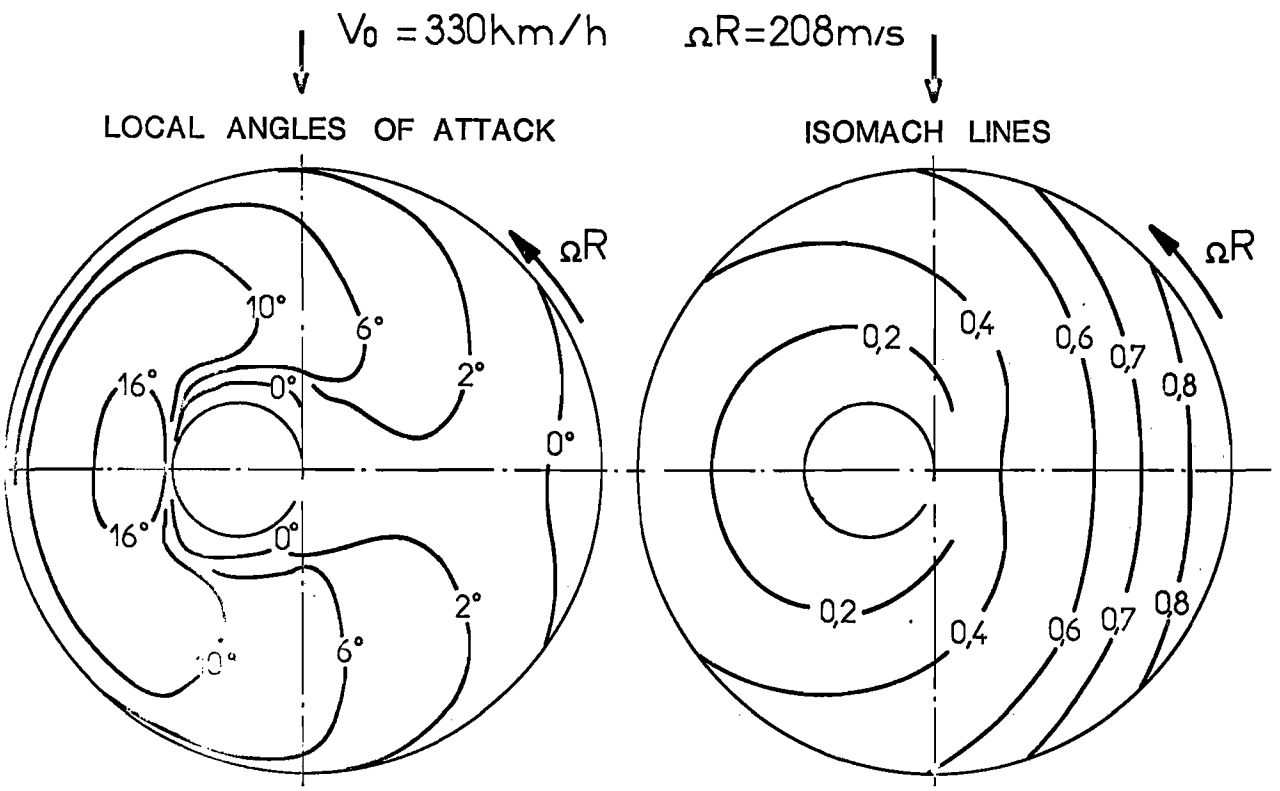

Fig. 3 – Typical Mach number and angle of attack distributions on the rotor disc in advancing flight.

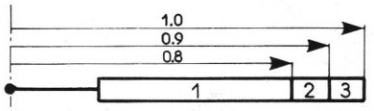

FLIGHT CONDITIONS	PREPONDERANT AERODYNAMIC COEFFICIENT		SECTIONS				
			1		2	3	
ADVANCING FLIGHT	Mdd at CL ~ 0	⩾	0.75	0.80	0.85	0.90	0.92
	$\|Cm_o\|$	⩽	0.01	0.01	0.01	0.01	0.01
HOVERING	L/D ratio at M_o ~ 0.5 - 0.6 CL = 0.6	⩾	80	75	80	85	85
MANEUVER	CL max Mo = 0.3	⩾		1.5	1.4		
	CL max Mo = 0.4	⩾	1.6		1.3	1.0	0.95
	CL max Mo = 0.5	⩾		1.3			
GEOMETRICAL CONSTRAINT t/C			13	12	9	7	6

Fig. 4 — Requirements for an helicopter blade.

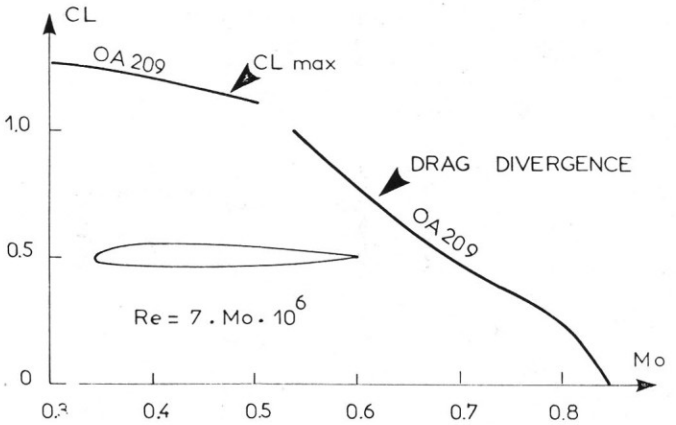

Fig. 5 — OA209 airfoil. Total performances.

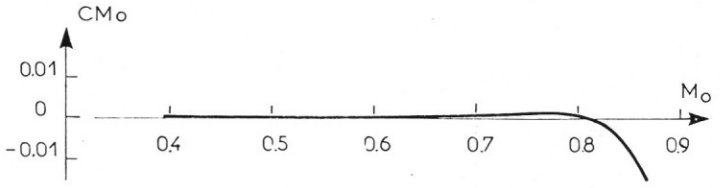

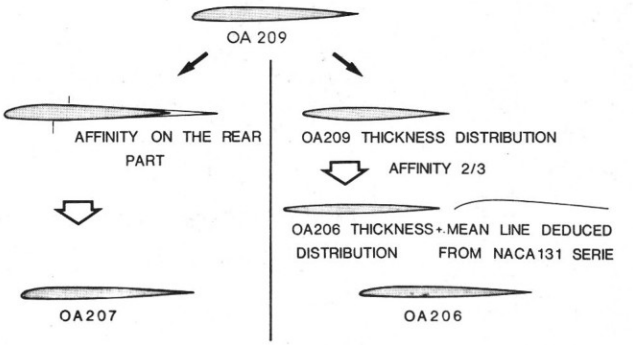

Fig. 6 — Airfoil design methodology for the tip sections of the blade.

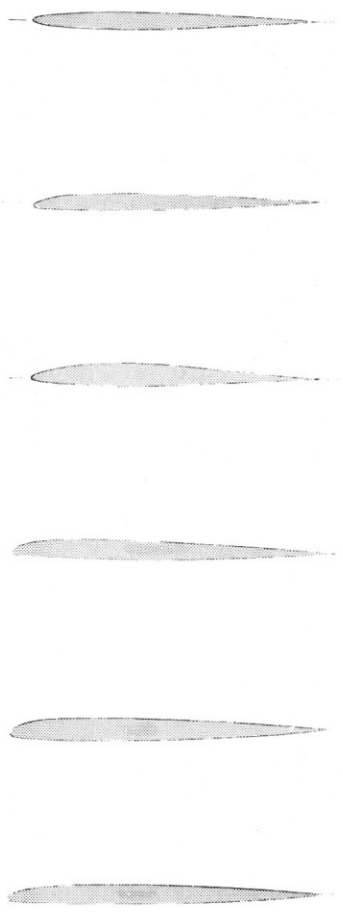

Fig. 7 – Contours of some thin airfoils.

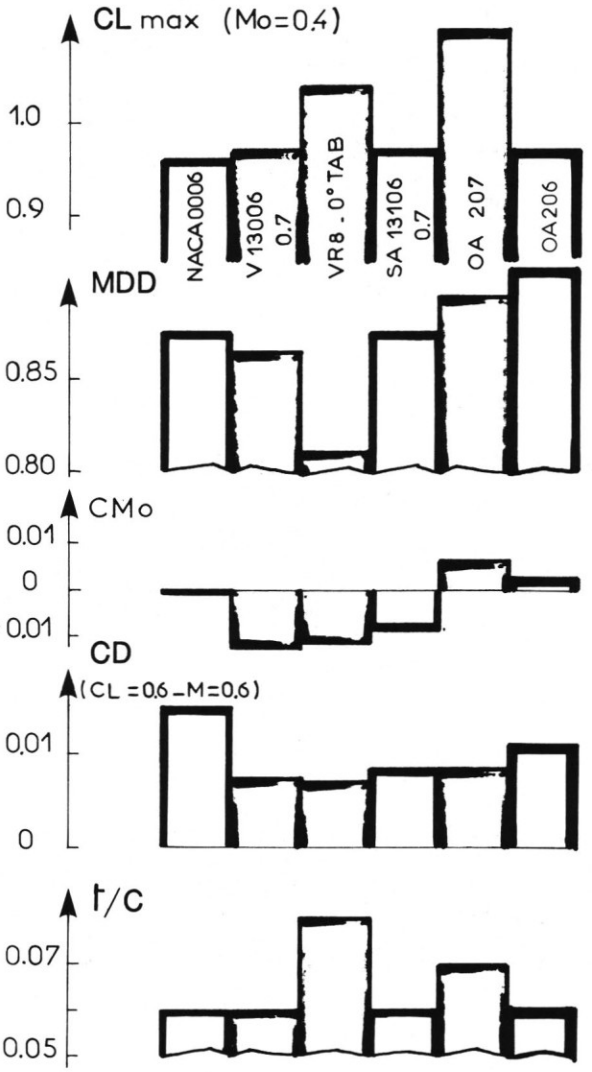

Fig. 8 – Comparison of the performances of some thin airfoils.

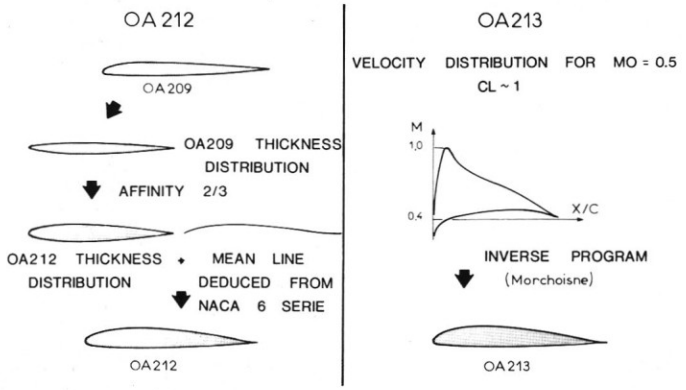

Fig. 9 – Airfoil design methodology for the inboard sections of the blade.

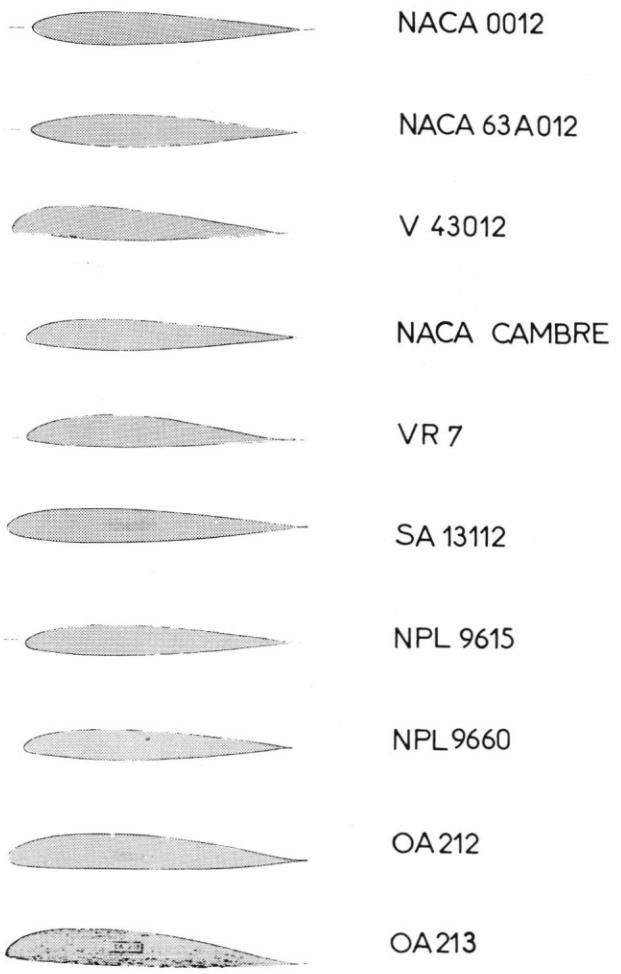

Fig. 10 – Contours of some ~12% thick airfoils.

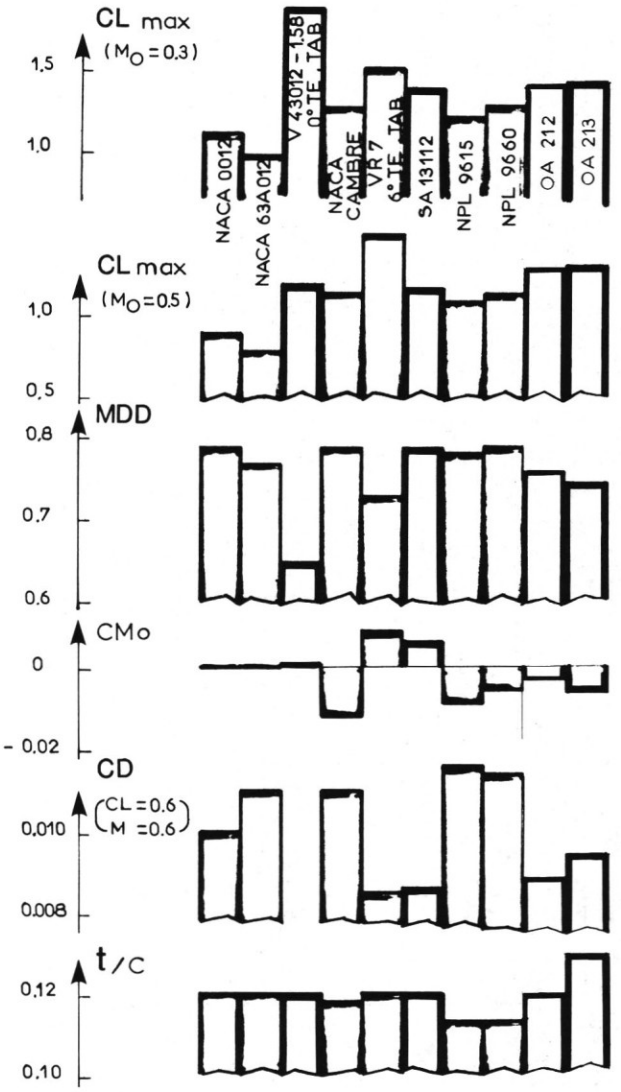

Fig. 11 – Comparison of the performances of some ~12% thick airfoils.

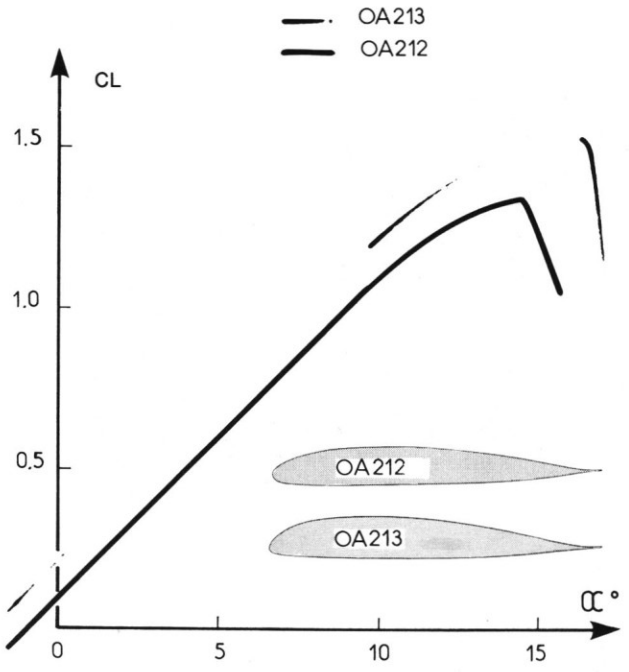

Fig. 12 – OA212 and OA213 airfoils. Lift curves at $M_o = 0.4$.

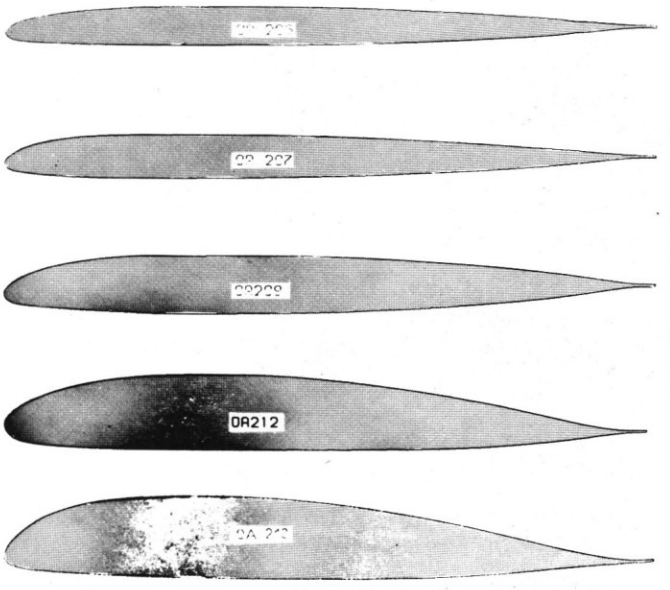

Fig. 13 – Contours of the OA airfoils family.

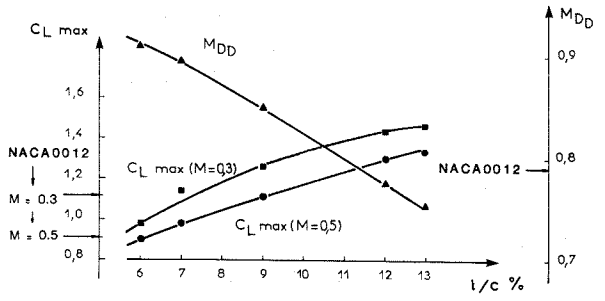

Fig. 14 — OA airfoils family. Total performances.

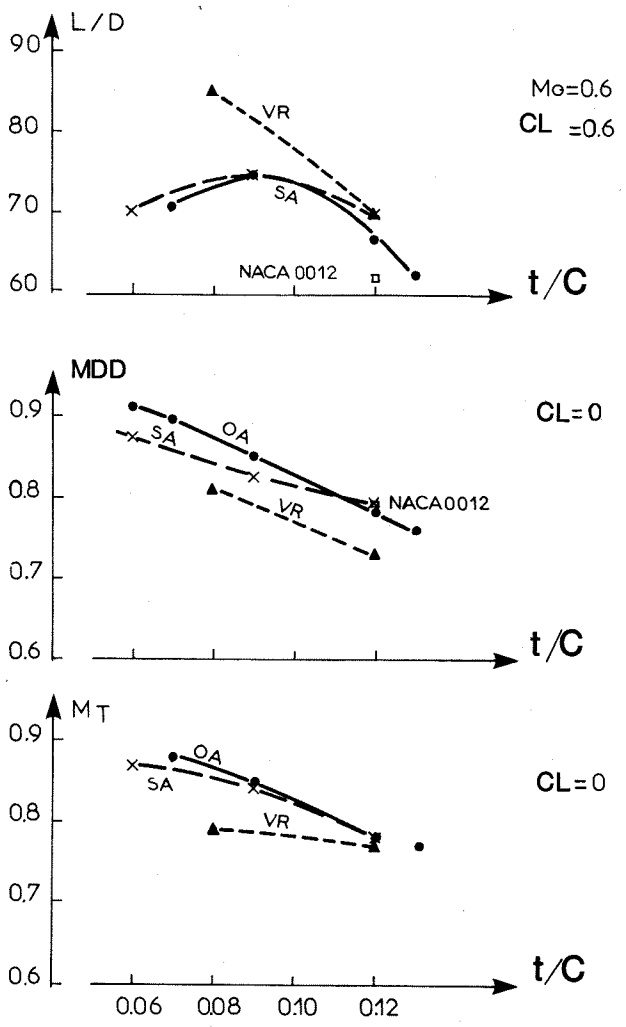

Fig. 16 — Comparison of the L/D, M_{dd} and Mach tuck of some airfoils families.

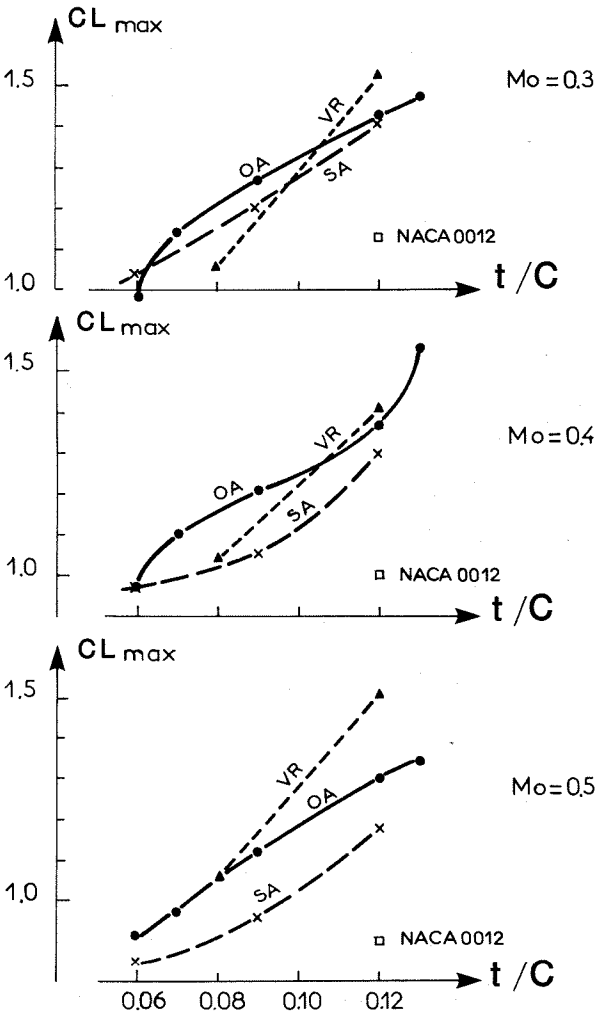

Fig. 15 — Comparison of the C_L max of some airfoils families.

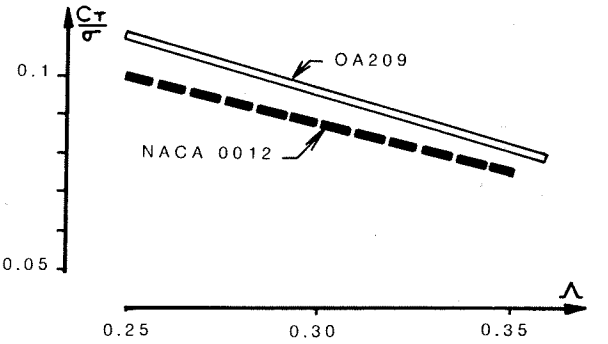

Fig. 17 — Increase of level flight envelope with OA209 airfoil.

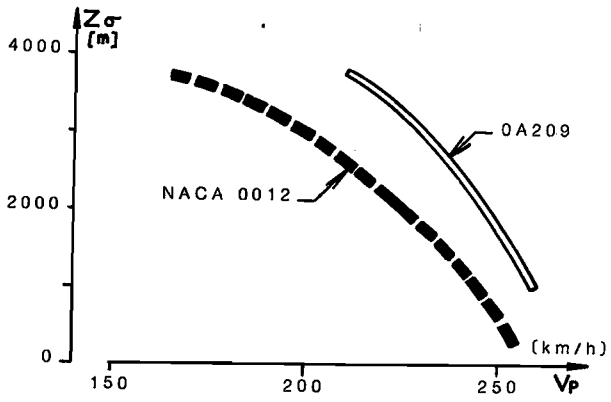

Fig. 18 – Increase of maximum level speed with OA209 airfoil.

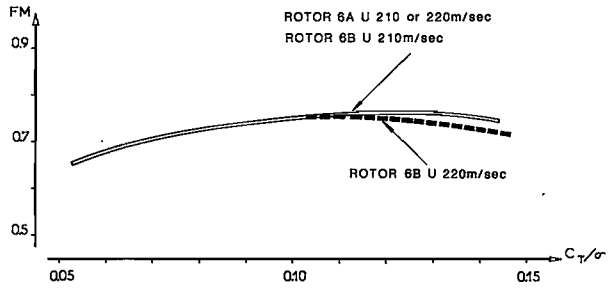

Fig. 21 – Influence of thickness tapering on rotor efficiency in hover.

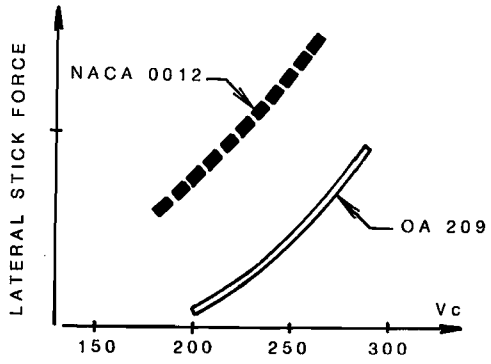

Fig. 19 – Airfoil influence on lateral stick force.

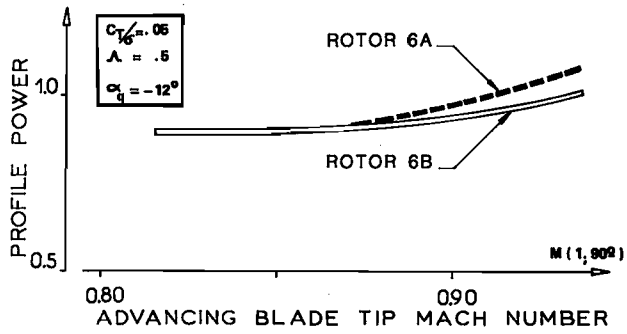

Fig. 22 – Effect of compressibility on OA airfoil rotors.

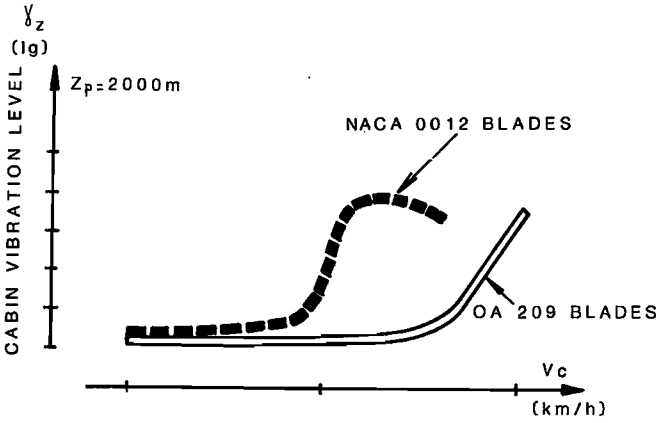

Fig. 20 – Airfoil influence on vibration level for high loaded rotor.

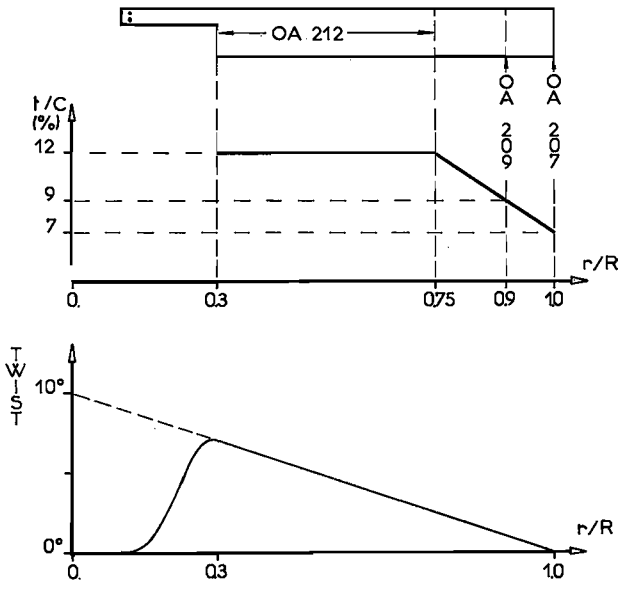

Fig. 23 – OA blade aerodynamic definition.

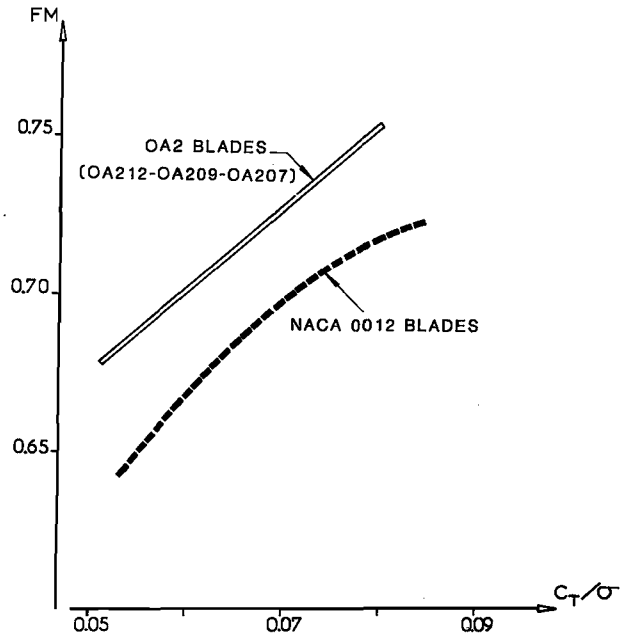

Fig. 24 — Influence of OA blades on rotor efficiency in hover (flight tests).

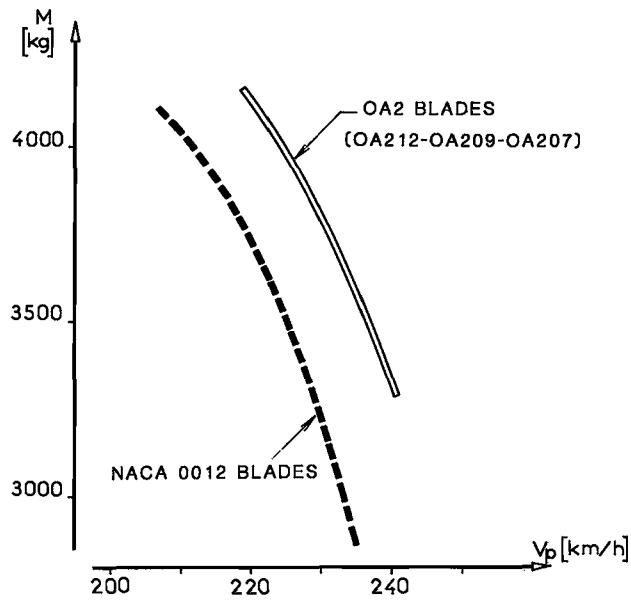

Fig. 25 — Performances of the OA blades in forward flight (flight tests).

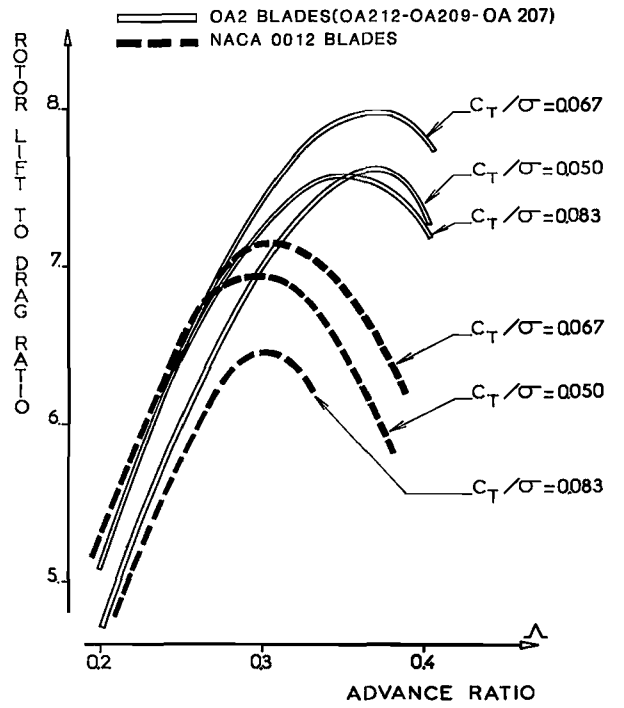

Fig. 26 — Influence of the OA blades on rotor lift to drag ratio (computation).

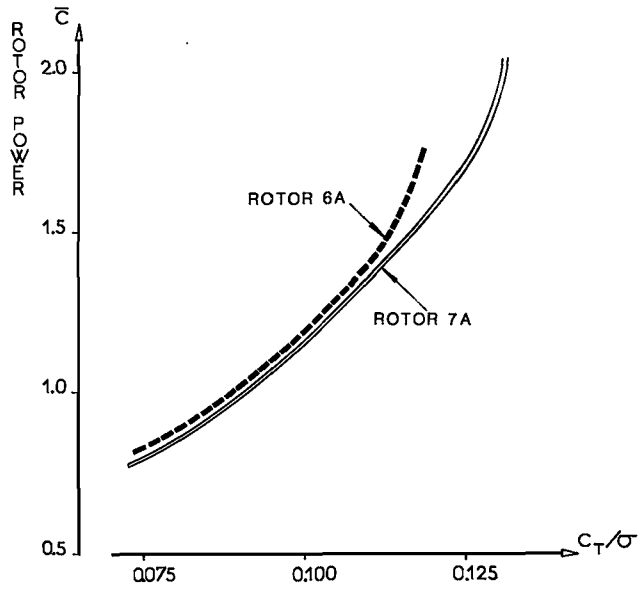

Fig. 27 — Influence of the OA213 section on rotor performance. (computation $\Lambda = 0.2 - \bar{X} = -1. - U = 210$ m/sec).

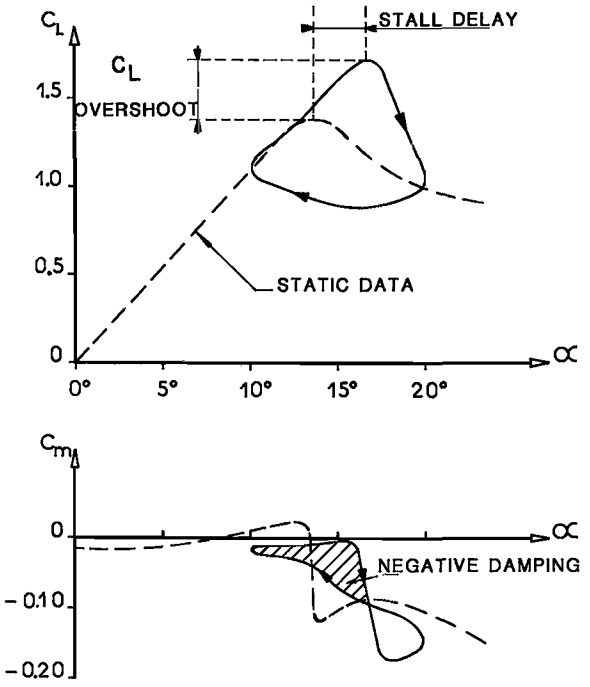

Fig. 28 – Three unsteady effects on rotor performance.